Supplementary Figures:

Figure S1

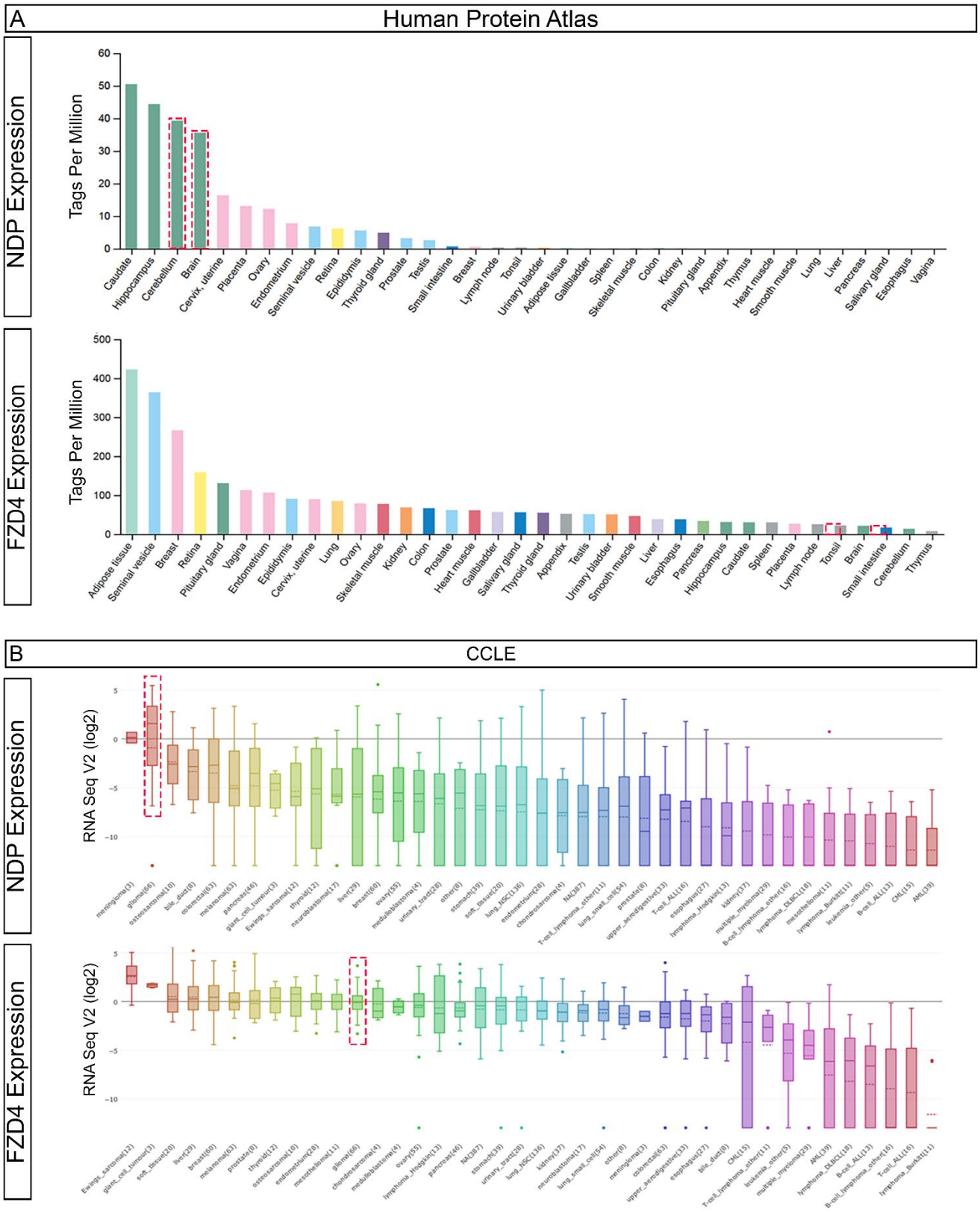


Figure S1. *NDP* expression is enriched in CNS tissues and GBM cell lines

(A) Analysis of The Functional Annotation of Mammalian Genomes 5 (FANTOM5) database using The Human Protein Atlas web server reveals an enrichment of *NDP* (top) but not *FZD* (bottom) expression in the CNS including brain and cerebellum tissues (top graph).

(B) Analysis of The Cancer Cell Line Encyclopedia (CCLE) reveals enrichment of *NDP* (upper) but not *FZD4* (bottom) expression in glioma cell lines (upper graph).

Figure S2

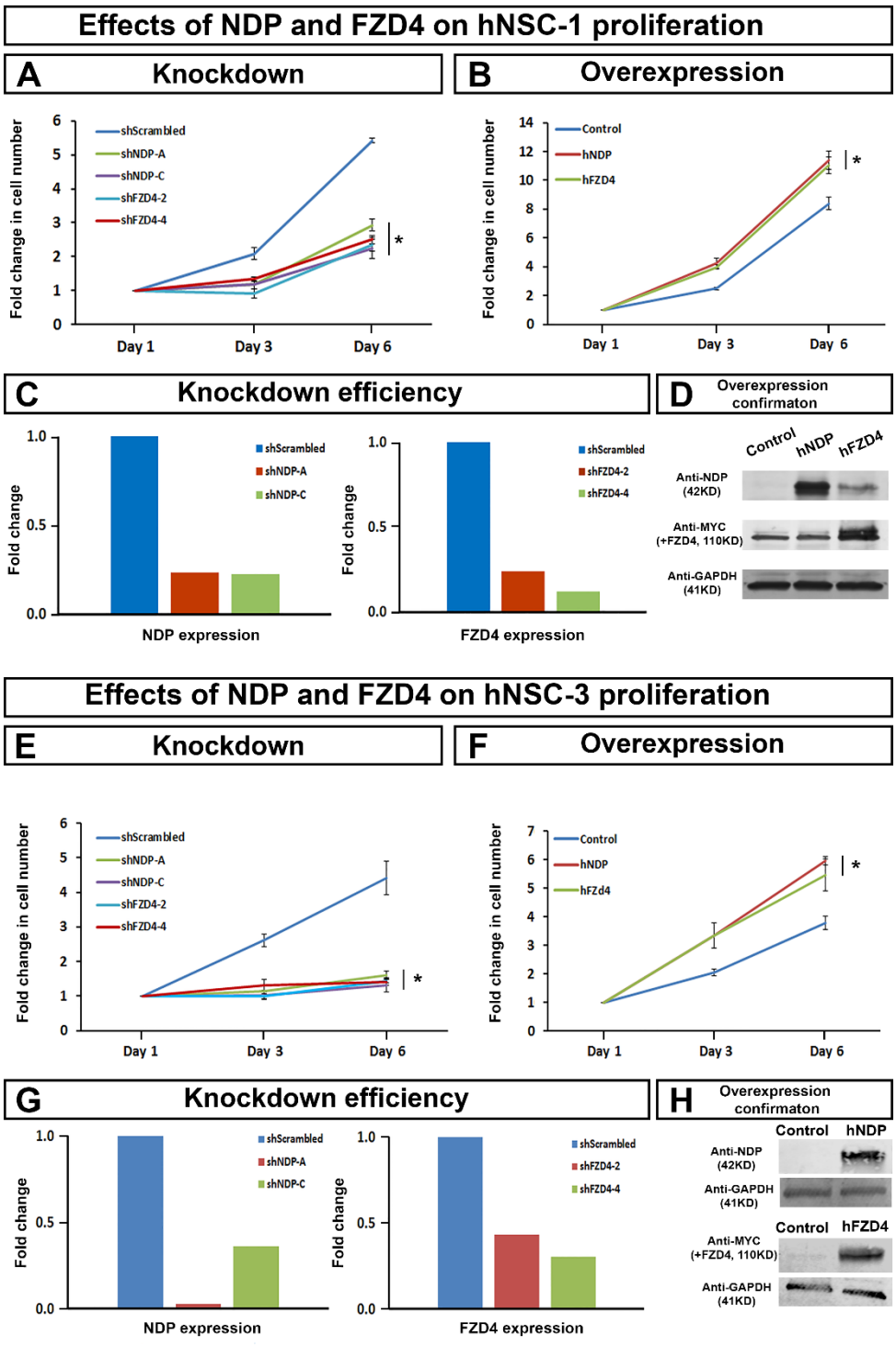

Effects of NDP and FZD4 on hNSC-1 proliferation
A Knockdown
B Overexpression
Fold change in cell number
shScrambled
shNDP-A
shNDP-C
shFZD4-2
shFZD4-4
Control
hNDP
hFZD4
Day 1
Day 3
Day 6
*
C Knockdown efficiency
D Overexpression confirmaton
Fold change
NDP expression
FZD4 expression
Control
hNDP
hFZD4
Anti-NDP (42KD)
Anti-MYC (+FZD4, 110KD)
Anti-GAPDH (41KD)
Effects of NDP and FZD4 on hNSC-3 proliferation
E Knockdown
F Overexpression
hFZd4
G Knockdown efficiency
H Overexpression confirmaton

Figure S2. *NDP* significantly promotes proliferation of hNSC cells in vitro

(A, E) Effect of *NDP* or *FZD4* knockdown (two independent shRNAs/gene) on the growth of hNSC-1 (A) and hNSC-3 (C) lines using the Trypan Blue proliferation assay after 3 and 6 days in culture. Knocking down *NDP* (green and violet lines) or *FZD4* (light blue and red lines) resulted in a significant inhibition of proliferation. n=3, error bars, mean ± SEM. Statistical significance (*) was tested using one-way ANOVA; $p < 0.05$.

(B, F) Effect of *NDP* (red line) or *FZD4* (green line) overexpression on hNSC-1 (B) or hNDC-3 (F) proliferation. n=3, error bars, mean ± SEM. Statistical significance (*) was tested using one-way ANOVA; $p < 0.05$.

(C, G) Representative replicates from qRT-PCR confirmation of knockdown efficiency of *NDP* or *FZD4* in hNSC-1 (C) or hNSC-3 (G).

(D, H) Western blot analysis to confirm overexpression in hNSC-1 (D) and hNSC-3 (H).

Figure S3

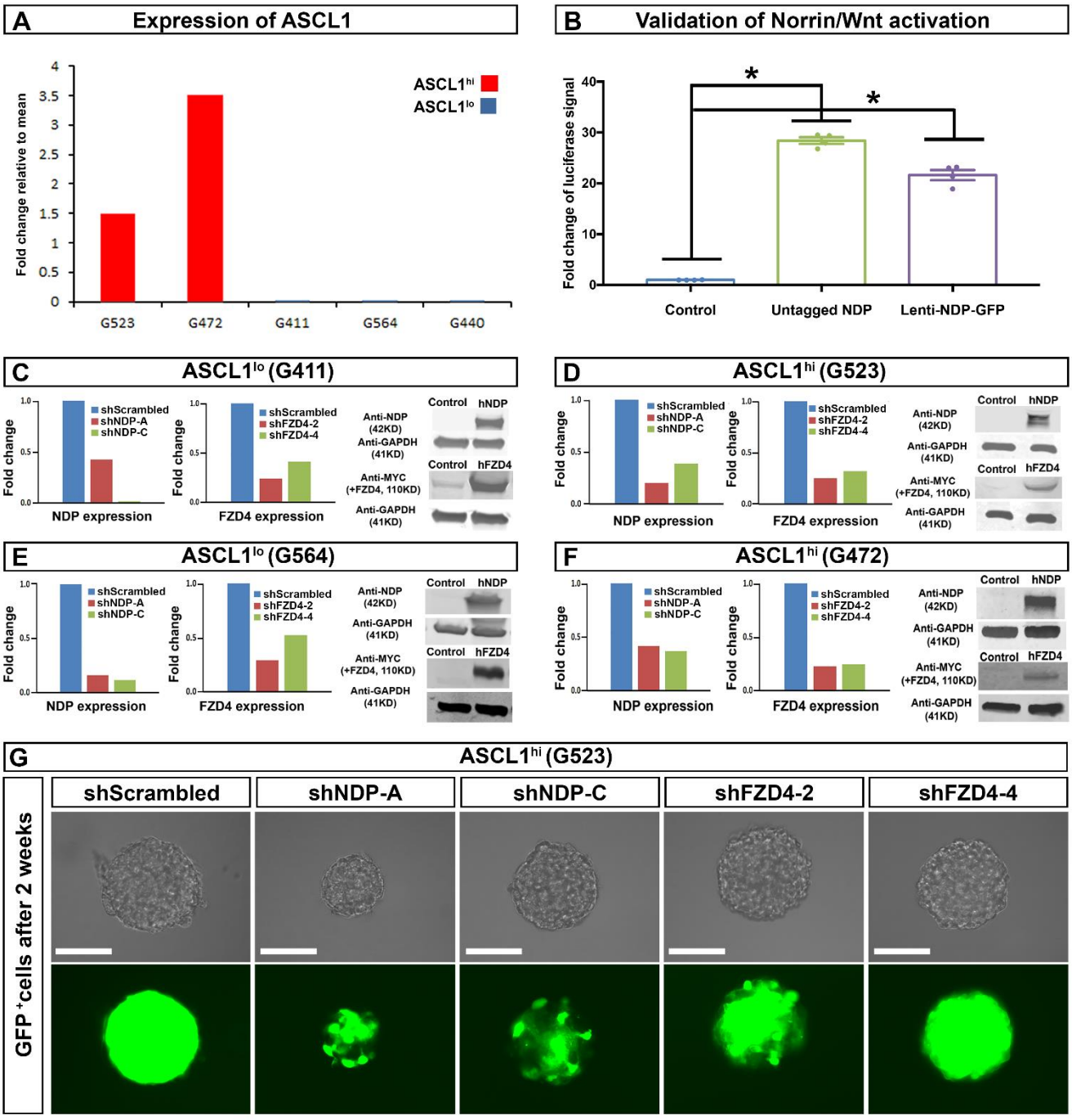

A
Expression of ASCL1
Fold change relative to mean
ASCL1hi
ASCL1lo
G523
G472
G411
G564
G440
B
Validation of Norrin/Wnt activation
Fold change of luciferase signal
Control
Untagged NDP
Lenti-NDP-GFP
C
ASCL1lo (G411)
D
ASCL1hi (G523)
E
ASCL1lo (G564)
F
ASCL1hi (G472)
shScrambled
shNDP-A
shNDP-C
shFZD4-2
shFZD4-4
NDP expression
FZD4 expression
Fold change
Anti-NDP (42KD)
Anti-GAPDH (41KD)
Anti-MYC (+FZD4, 110KD)
Control
hNDP
hFZD4
G
ASCL1hi (G523)
shScrambled
shNDP-A
shNDP-C
shFZD4-2
shFZD4-4
GFP+cells after 2 weeks

Figure S3. Confirming knockdown and overexpression efficiency in all GSC lines

(A) qRT-PCR analysis confirming the *ASCL1* expression in the GSC lines used in this study. G523 and G472 (red bars) are confirmed to be $ASCL1^{hi}$, while G411, G564 and G440 (blue bars) belong to the $ASCL1^{lo}$ subtype.

(B) Validating the activity of untagged- and GFP-tagged NDP overexpressing plasmids on B-catenin Top-Flash luciferase reporter assay. Statistical significance (*) was tested using one-way ANOVA; $p<0.05$.

(C-F) Representative replicates from qRT-PCR analysis of knockdown efficiency for *NDP* or *FZD4*, and western blotting analysis to confirm overexpression in G411 (C), G523 (D), G564 (E), G472 (F) GSC lines. Note: the blots presented in (F) are retrieved from samples run on parallel gels.

(G) GFP+ cells in spheres from G523 GSCs after *NDP* and FZD4 knockdown. Spheres from GSCs with *NDP* knockdown exhibit lower levels of GFP, Scale bar, 50 μM.

Figure S4

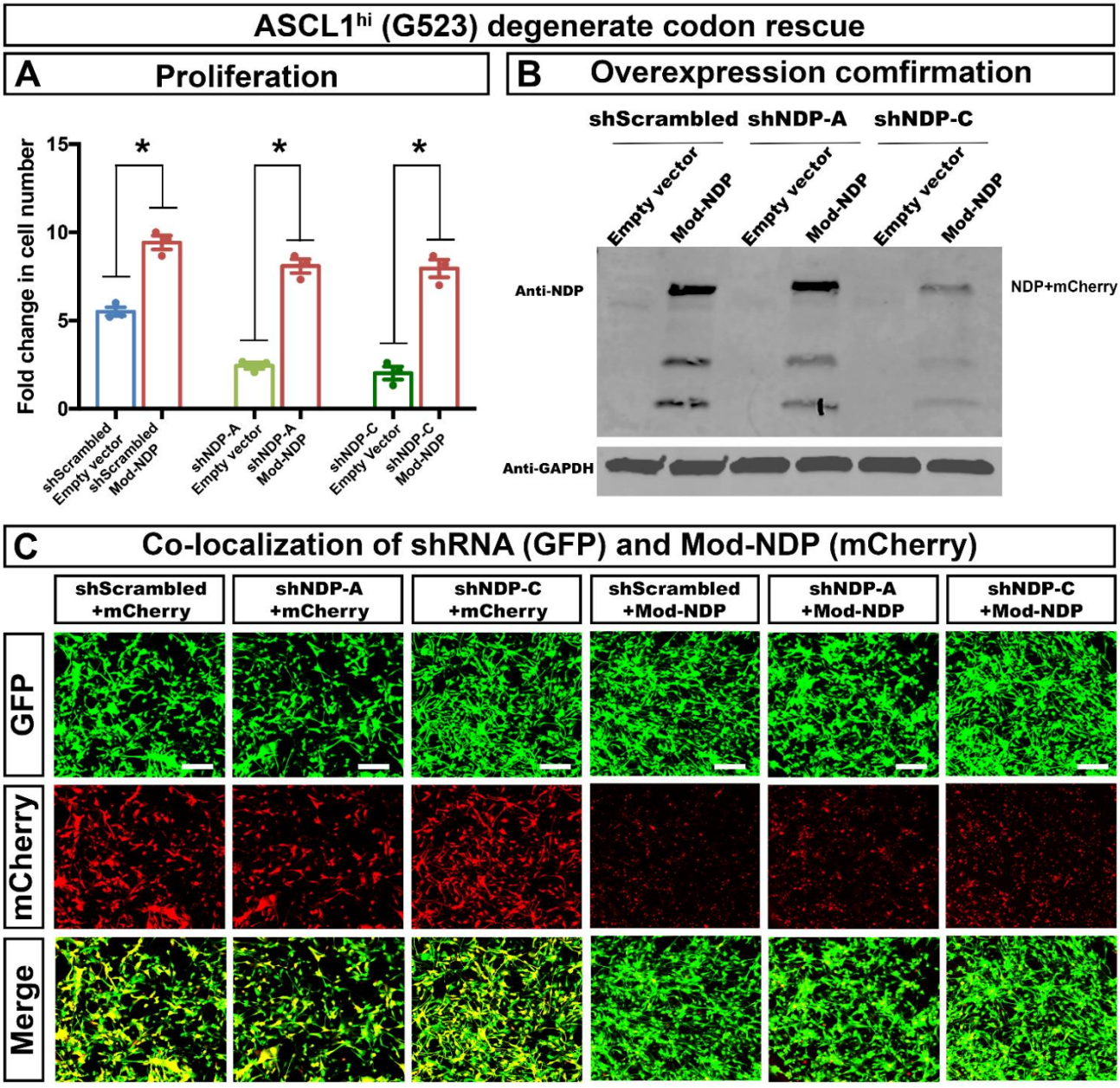

ASCL1hi (G523) degenerate codon rescue
A Proliferation
B Overexpression comfirmation
Fold change in cell number
15
10
5
0
*
*
*
shScrambled Empty vector
shScrambled Mod-NDP
shNDP-A Empty vector
shNDP-A Mod-NDP
shNDP-C Empty Vector
shNDP-C Mod-NDP
shScrambled
shNDP-A
shNDP-C
Empty vector
Mod-NDP
Anti-NDP
NDP+mCherry
Anti-GAPDH
C Co-localization of shRNA (GFP) and Mod-NDP (mCherry)
shScrambled +mCherry
shNDP-A +mCherry
shNDP-C +mCherry
shScrambled +Mod-NDP
shNDP-A +Mod-NDP
shNDP-C +Mod-NDP
GFP
mCherry
Merge

Figure S4. Overexpression of shNDP-insensitive *NDP* rescues the observed effects of *NDP* knockdown

(A) *NDP* knockdown G523 cells were transduced with a modified degenerate codon version of *NDP* (Mod-NDP) to express shRNA-insensitive version of *NDP*, then cell growth was assessed using the Trypan blue proliferation assay. Mod-NDP was able to rescue the effects of *NDP* knockdown on proliferation, validating the specificity of our *NDP* shRNAs. n=3, error bars, mean ± SEM. Statistical significance (*) was tested using one-way ANOVA; $p < 0.05$.

(B) Western blot confirmation of Mod-NDP overexpression.

(C) Co-localization of *NDP* knockdown (GFP+) and Mod-NDP (mCherry+) in G523 GSCs after double infection. Scale bar, 50 μM.

Figure S5

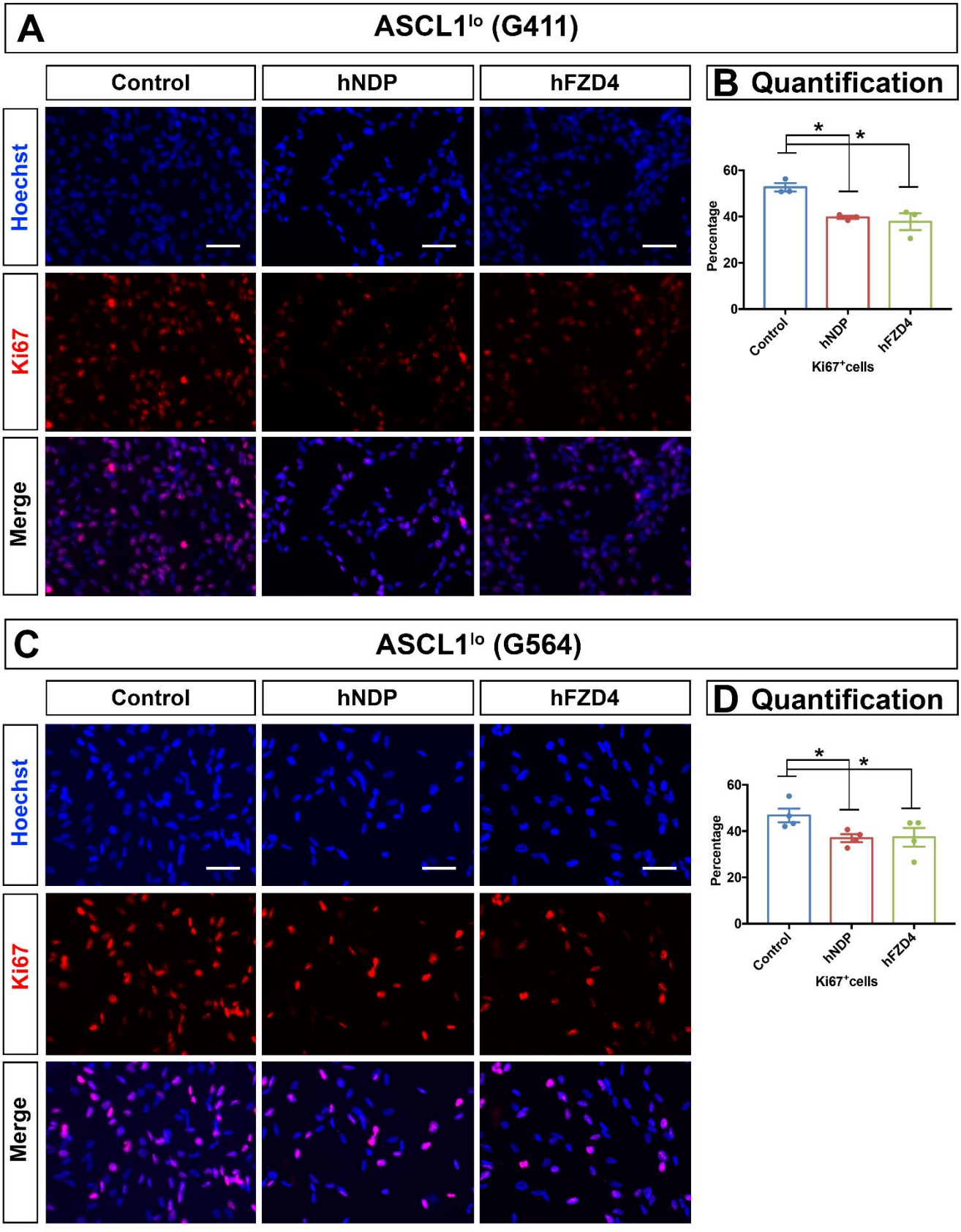

A
ASCL1lo (G411)
Control
hNDP
hFZD4
Hoechst
Ki67
Merge
B Quantification
Percentage
60
40
20
0
*
*
Control
hNDP
hFZD4
Ki67+cells
C
ASCL1lo (G564)
Control
hNDP
hFZD4
Hoechst
Ki67
Merge
D Quantification
Percentage
60
40
20
0
*
*
Control
hNDP
hFZD4
Ki67+cells

Figure S5. Overexpression of *NDP* or *FZD4* results in a significant decrease in the proliferative population in ASCL1^{lo} GSCs

(A, C) Representative images of ICC staining for Ki67 (red) after *NDP* or *FZD4 overexpression* in G411 (A) and G564 (B) (ASCL1^{lo}) cells. Overexpressing *NDP* or *FZD4* resulted in a significant decrease in Ki67+ cells. Scale bar, 50 μM.

(B, D) Quantification of the Ki67+ cell population in G411 (C) and G564 (D) after *NDP* or *FZD4* overexpression. n=3, 4 respectively, error bars, mean ± SEM. Statistical significance (*) was tested using one-way ANOVA; $p < 0.05$.

Figure S6

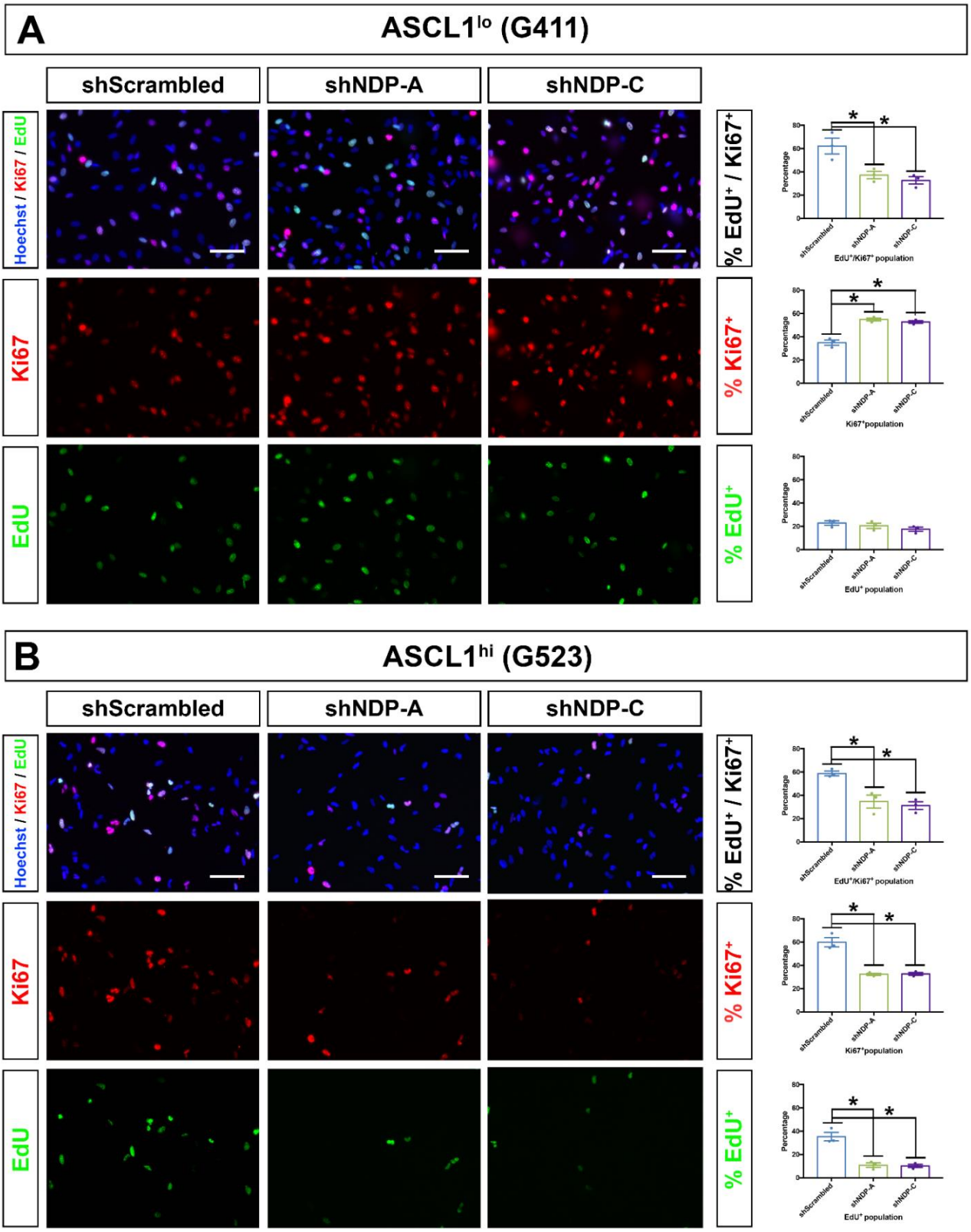

A
ASCL1lo (G411)
shScrambled
shNDP-A
shNDP-C
Hoechst / Ki67 / EdU
Ki67
EdU
% EdU+ / Ki67+
% Ki67+
% EdU+
Percentage
EdU+/Ki67+ population
Ki67+population
EdU+ population
B
ASCL1hi (G523)
shScrambled
shNDP-A
shNDP-C
Hoechst / Ki67 / EdU
Ki67
EdU
% EdU+ / Ki67+
% Ki67+
% EdU+
Percentage
EdU+/Ki67+ population
Ki67+population
EdU+ population

Figure S6. Knocking down *NDP* slows cell cycle progression in both ASCL1^{lo} and ASCL1^{hi} GSCs

(A) ICC staining for Ki67 (red) and EdU (green) after *NDP* knockdown in G411 (ASCL1^{lo}) cells. Knocking down *NDP* or *FZD4* leads to a significant increase in the frequency of Ki67^{+} cells and a reduction in the frequency of EdU^{+}/Ki67+ cells. Scale bar, 50 μM. Quantification of respective stains is included in the right panel. n=3, error bars, mean ± SEM. Statistical significance (*) was tested using one-way ANOVA; $p < 0.05$.

(B) ICC staining for Ki67 (red) and EdU (green) after *NDP* knockdown in G523 (ASCL1^{hi}) cells. Knocking down *NDP* or *FZD4* leads to a significant decrease in the frequency of Ki67^{+} and EdU^{+}/Ki67+ cells. Scale bar, 50 μM. Quantification of respective stains is included in the right panel. n=3, error bars, mean ± SEM. Statistical significance (*) was tested using one-way ANOVA; $p < 0.05$.

Figure S7

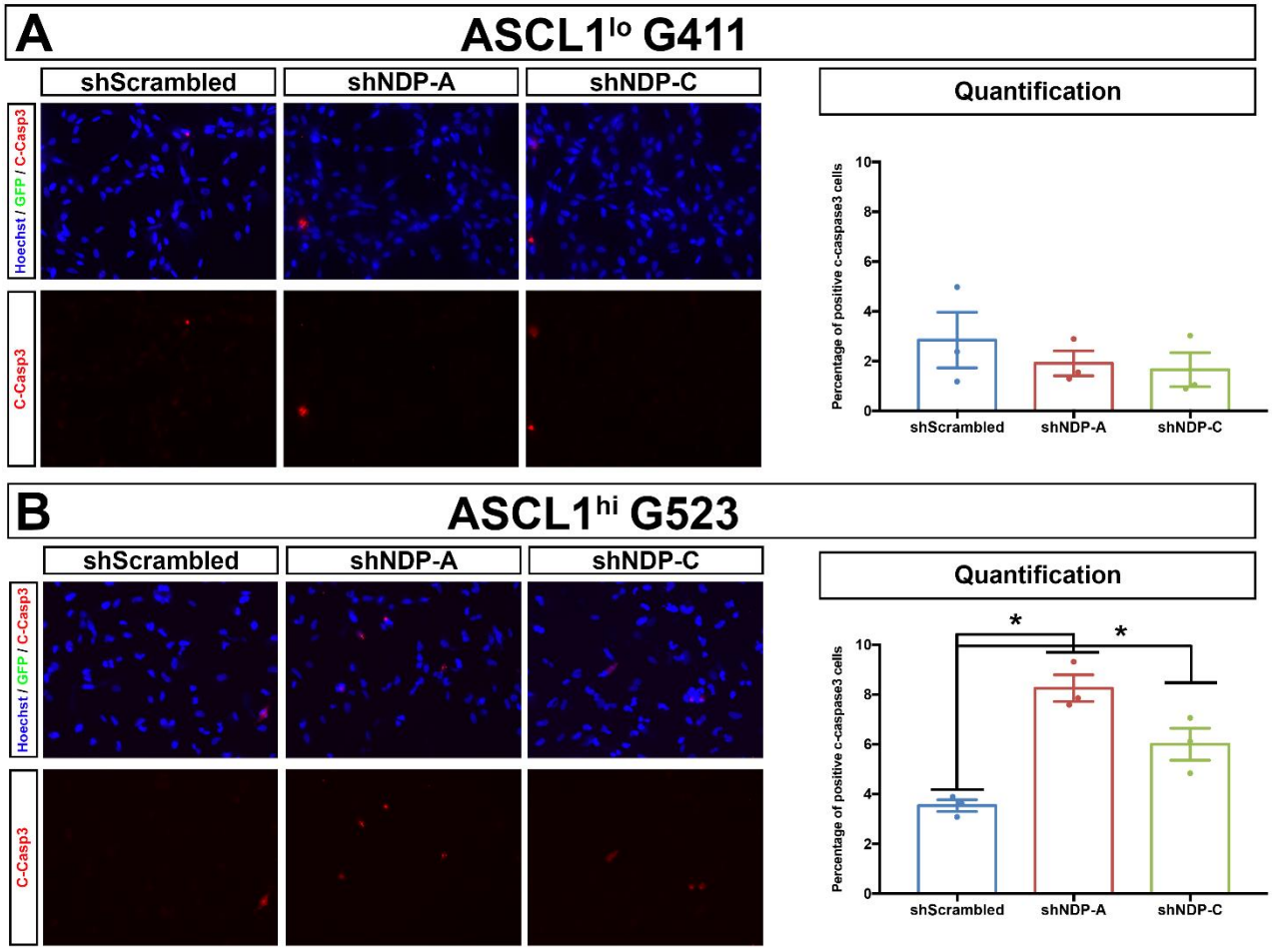

A
ASCL1lo G411
shScrambled
shNDP-A
shNDP-C
Hoechst / GFP / C-Casp3
C-Casp3
Quantification
Percentage of positive c-caspase3 cells
shScrambled
shNDP-A
shNDP-C
B
ASCL1hi G523
shScrambled
shNDP-A
shNDP-C
Hoechst / GFP / C-Casp3
C-Casp3
Quantification
*
*
Percentage of positive c-caspase3 cells
shScrambled
shNDP-A
shNDP-C

Figure S7. *NDP* knockdown increases the percentage of apoptotic cells in ASCL1^{hi} but not ASCL1^{lo} GSCs in vitro

(A) ICC quantification of cleaved-Caspase 3 (red) 4 days after *NDP* knockdown in G411. Scale bar, 50 μM. Statistical significance (*) was tested using one-way ANOVA; $p<0.05$.

(B) ICC quantification of cleaved-Caspase 3 (red) 4 days after *NDP* knockdown in G523. Scale bar, 50 μM. Statistical significance (*) was tested using one-way ANOVA; $p<0.05$.

Figure S8

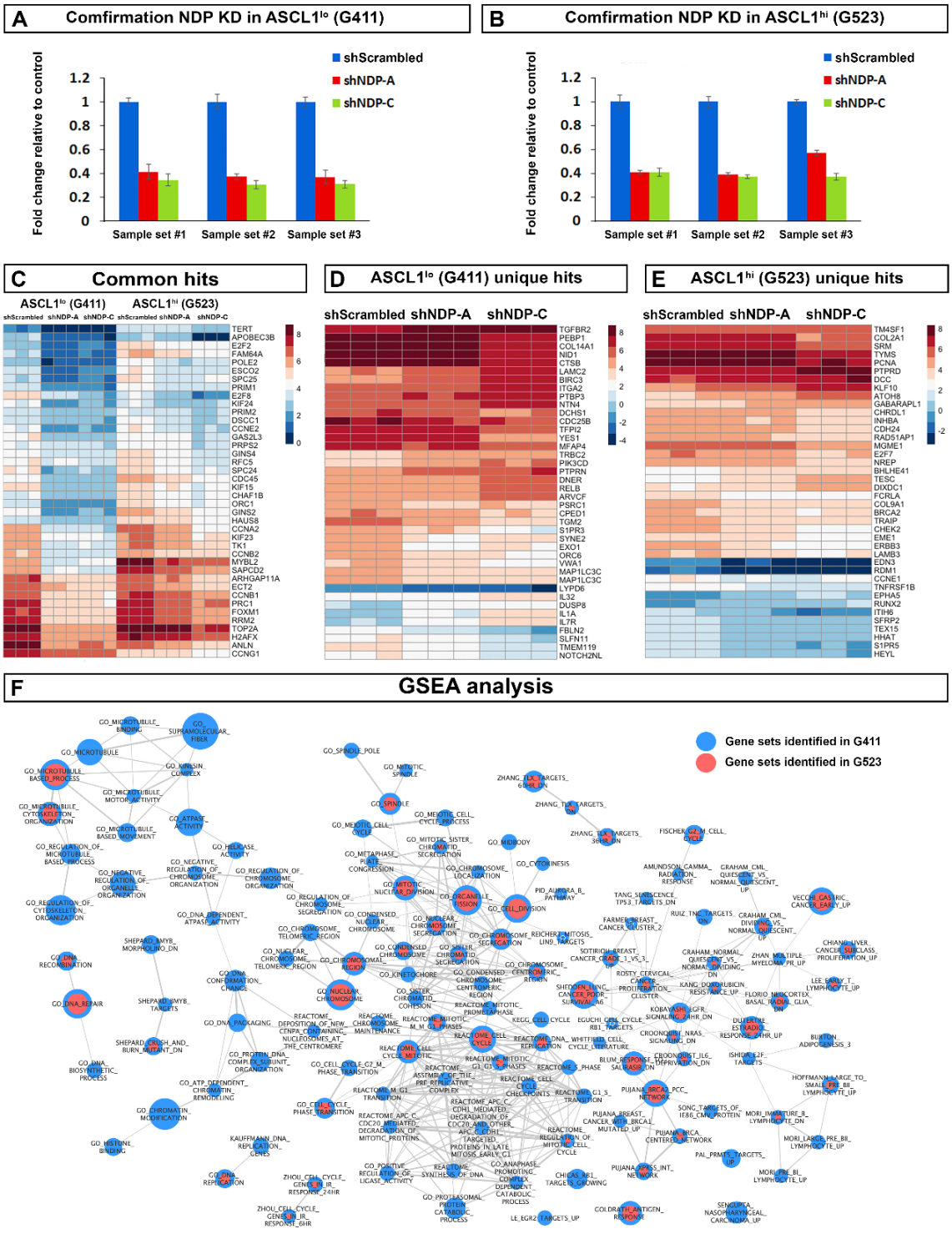

A
Comfirmation NDP KD in ASCL1lo (G411)
B
Comfirmation NDP KD in ASCL1hi (G523)
Fold change relative to control
shScrambled
shNDP-A
shNDP-C
Sample set #1
Sample set #2
Sample set #3
C
Common hits
ASCL1lo (G411)
ASCL1hi (G523)
D
ASCL1lo (G411) unique hits
E
ASCL1hi (G523) unique hits
F
GSEA analysis
Gene sets identified in G411
Gene sets identified in G523

Figure S8. Details of the RNA-Seq and GSEA analysis

(A, B) Confirmation of *NDP* knockdown in samples that were used for RNA-Seq library from G411 (A) and G523 (B) cells. Error bars represent differences among the biological replicates.

(C-E) Heatmaps of some differentially expressed genes after *NDP* knockdown in both cell lines.

(F) Detailed unbiased enrichment maps of the identified hits in both lines (blue circles, G411, red circles, G523). Interestingly, the overlapping gene sets predominantly center on cell cycle, cell division and proliferation, while gene sets unique to G411 are related to cytoskeleton re-arrangement and cell movement.

Figure S9

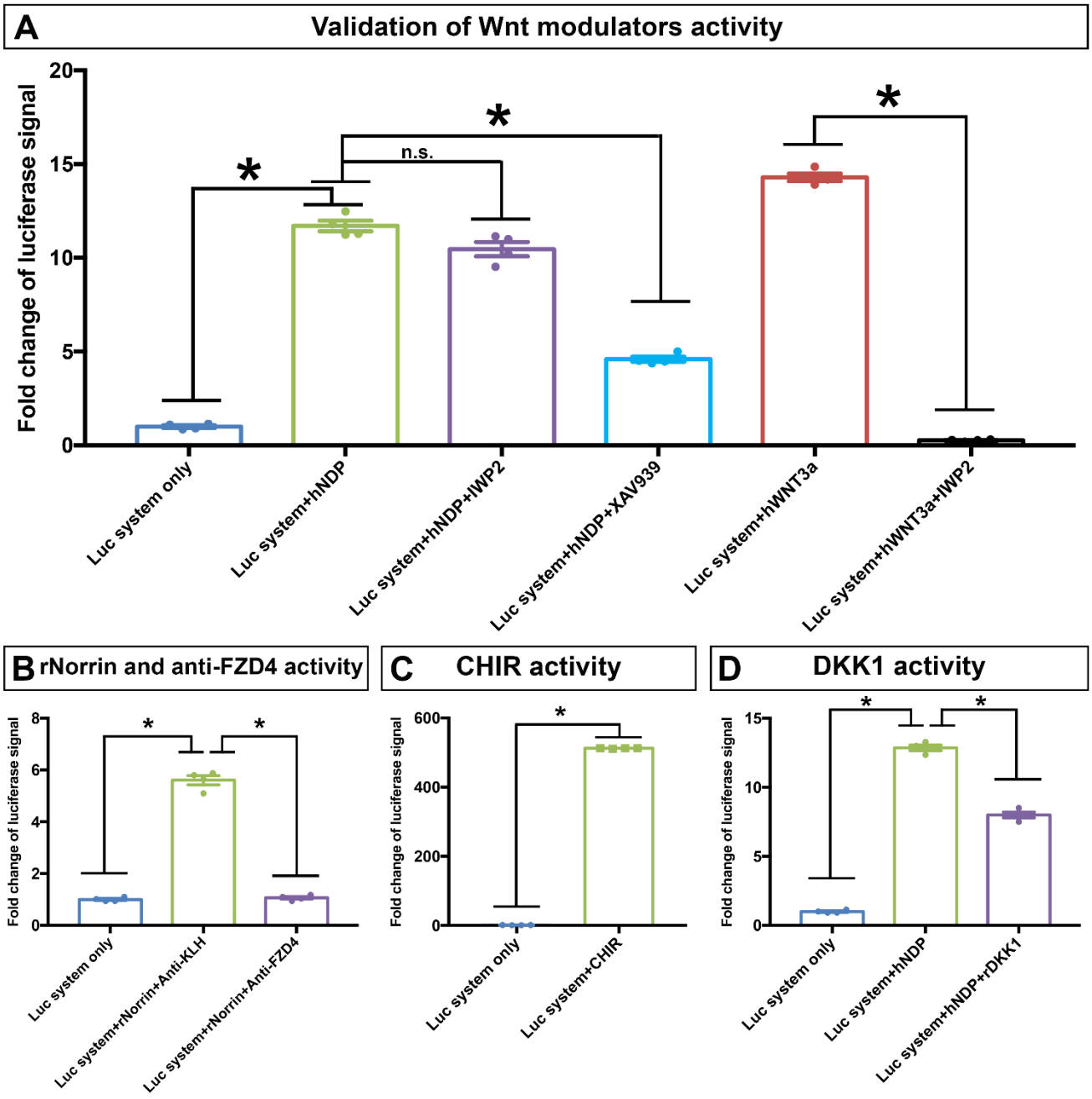

A
Validation of Wnt modulators activity
Fold change of luciferase signal
20
15
10
5
0
*
*
*
n.s.
Luc system only
Luc system+hNDP
Luc system+hNDP+IWP2
Luc system+hNDP+XAV939
Luc system+hWNT3a
Luc system+hWNT3a+IWP2
B
rNorrin and anti-FZD4 activity
Fold change of luciferase signal
8
6
4
2
0
*
*
Luc system only
Luc system+rNorrin+Anti-KLH
Luc system+rNorrin+Anti-FZD4
C
CHIR activity
Fold change of luciferase signal
600
400
200
0
*
Luc system only
Luc system+CHIR
D
DKK1 activity
Fold change of luciferase signal
15
10
5
0
*
*
Luc system only
Luc system+hNDP
Luc system+hNDP+rDKK1

Figure S9. Validation of Wnt modulators in Top-Flash luciferase reporter assay

(A) Validating the activity of Wnt inhibitors in inhibiting *NDP*-induced Wnt signaling in HEK293T cells using B-catenin Top-Flash reporter assay. Notably, IWP2 does not seem to inhibit the activity of NDP, so we used WNT3a as a stimulator to for basal system activation (last two bars in the graph). n=4, error bars, mean ± SEM. Statistical significance (*) was tested using one-way ANOVA; $p < 0.05$.

(B) Validating the of recombinant human Norrin and anti-FZD4 blocking antibody in HEK293T cells using B-catenin Top-Flash reporter assay. n=4, error bars, mean ± SEM. Statistical significance (*) was tested using one-way ANOVA; $p < 0.05$.

(C) Validating the activity of the CHIR (small molecule inhibitor of GSK-3B) in HEK293T cells using B-catenin Top-Flash reporter assay. n=4, error bars, mean ± SEM. Statistical significance (*) was tested using Student's t-test; $p < 0.05$.

(D) Validating the activity of recombinant DKK1 in inhibiting *NDP*-induced Wnt signaling in HEK293T cells using B-catenin Top-Flash reporter assay. n=4, error bars, mean ± SEM. Statistical significance (*) was tested using one-way ANOVA; $p < 0.05$.

Figure S10

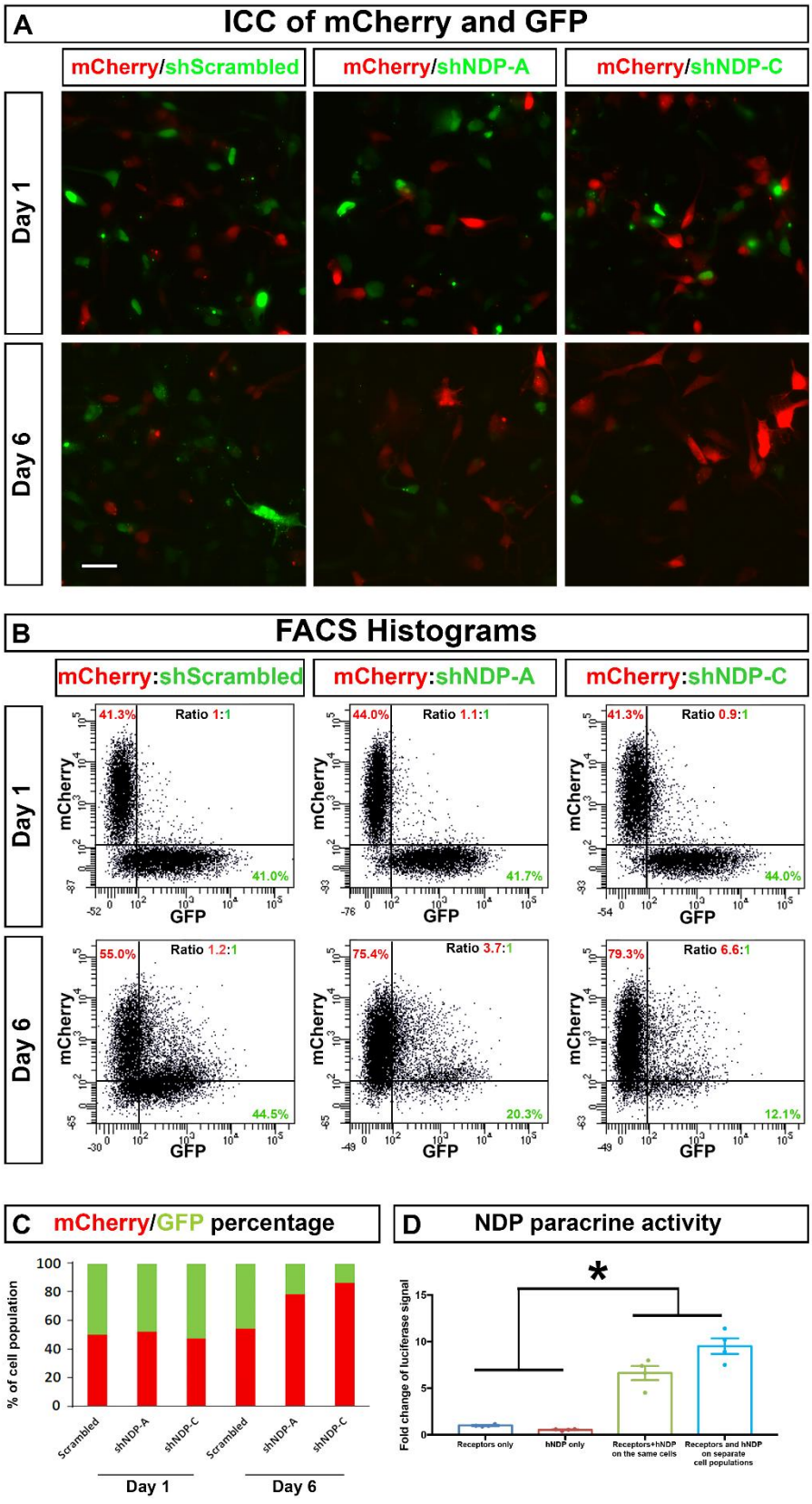

A
ICC of mCherry and GFP
mCherry/shScrambled
mCherry/shNDP-A
mCherry/shNDP-C
Day 1
Day 6
B
FACS Histograms
mCherry:shScrambled
mCherry:shNDP-A
mCherry:shNDP-C
Day 1
Day 6
41.3%
Ratio 1:1
41.0%
44.0%
Ratio 1.1:1
41.7%
41.3%
Ratio 0.9:1
44.0%
55.0%
Ratio 1.2:1
44.5%
75.4%
Ratio 3.7:1
20.3%
79.3%
Ratio 6.6:1
12.1%
mCherry
GFP
C
mCherry/GFP percentage
% of cell population
Scrambled
shNDP-A
shNDP-C
Day 1
Day 6
D
NDP paracrine activity
Fold change of luciferase signal
Receptors only
hNDP only
Receptors+hNDP on the same cells
Receptors and hNDP on separate cell populations

Figure S10. *NDP* mediates ASCL1^{hi} GSC proliferation through a cell autonomous, and not a paracrine mechanism

(A) Representative images of G523 (ASCL1^{hi}) (GFP+) expressing shScrambled, shNDP-A, shNDP-C, which were mixed with wild-type G523 (mCherry+) cells in 1:1: ratio at day 1 and day 6 in culture. Histograms representing one replicate. The GFP+ cell population underwent a striking reduction in shNDP-A or shNDP-C expressing co-cultures cells, relative to shScrambled co- cultures. Notably, there was a strong growth selective disadvantage of the GFP+ cells at day 6 in both *NDP* knockdown constructs. Magnification 20X. Scale bar, 50 μM.

(B) Histograms representing FACS-quantified percentages of wildtype (mCherry+) G523: NDP knockdown (GFP+) G523 cells at day 1 and day 6. The GFP+ cell population underwent a striking reduction by day 6 after *NDP* knockdown.

(C) Graphical representation of changes of cellular ratio in one representative replicate.

(D) Confirmation of paracrine signaling for NDP activation of TOP-Flash in HEK293T cells. n=4, error bars, mean ± SEM. Statistical significance (*) was tested using one-way ANOVA; $p < 0.05$.

Figure S11

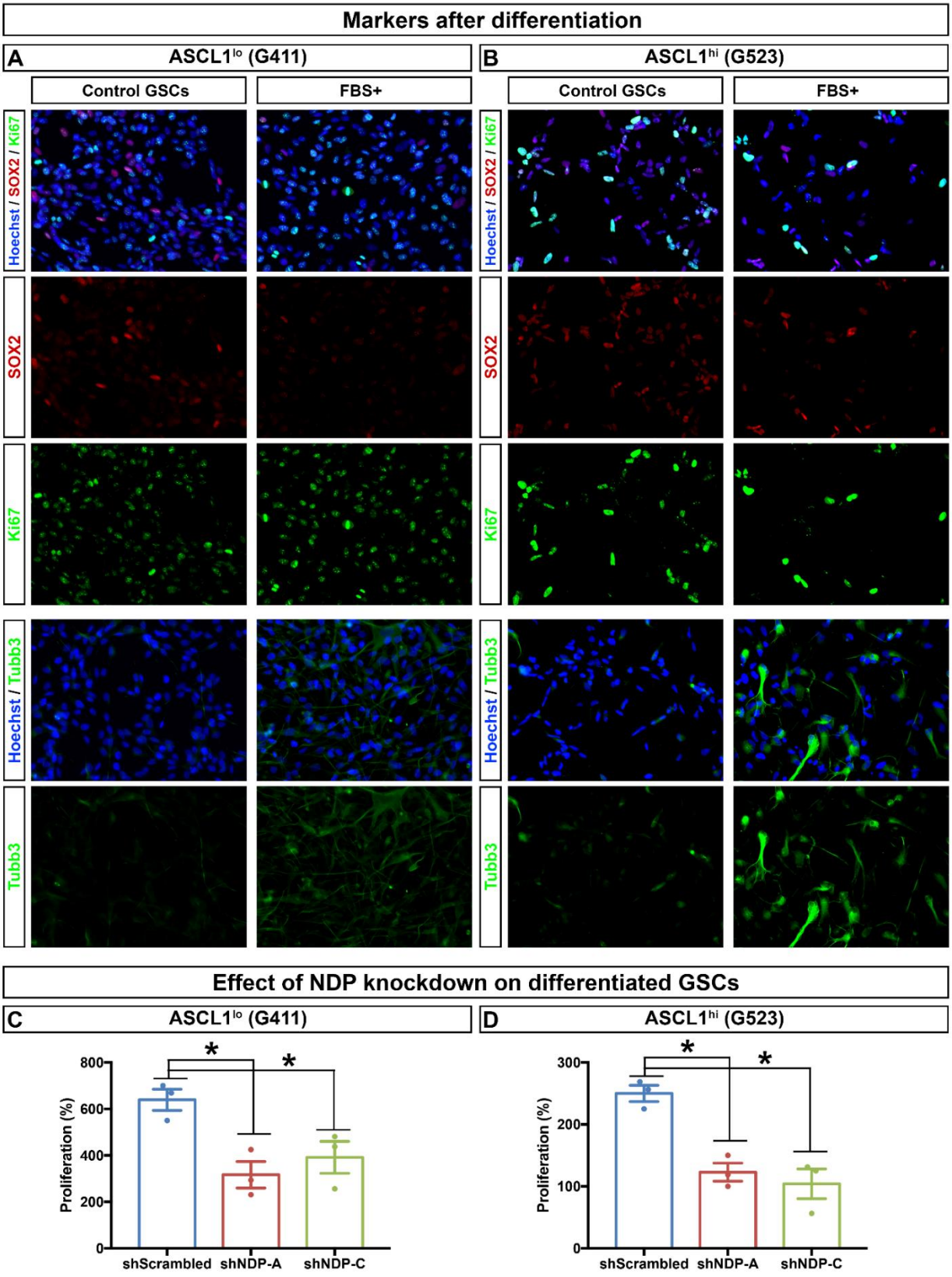

Markers after differentiation
A
ASCL1lo (G411)
B
ASCL1hi (G523)
Control GSCs
FBS+
Hoechst / SOX2 / Ki67
SOX2
Ki67
Hoechst / Tubb3
Tubb3
Effect of NDP knockdown on differentiated GSCs
C
ASCL1lo (G411)
D
ASCL1hi (G523)
Proliferation (%)
800
600
400
200
0
300
100
*
shScrambled
shNDP-A
shNDP-C

Figure S11. Effects of *NDP* knockdown on serum-differentiated GSCs proliferation in vitro

(A, B) Representative images from ICC staining of stem cell (SOX2), differentiation (BIII-TUBB) and proliferation (Ki67) markers in G411 and G523 cells after differentiation for 1 week in FBS-supplemented culture. Scale bar, 50 μM.

(C, D) Effect of *NDP* knockdown on proliferation of serum-differentiated G411 (C) and G523 (D) after 3 days in culture. Statistical significance (*) was tested using one-way ANOVA; $p < 0.05$.

Supplementary Tables

Table S1.

Cell type	NDP KD		NDP OE		FZD4 KD		FZD4 OE	
	Growth	Sphere	Growth	Sphere	Growth	Sphere	Growth	Sphere
hNSC (hNSC-1, hNSC-3)	↓	Untested	↑	Untested	↓	Untested	↑	Untested
ASCL1^{lo} GNS (G411, G564)	↑	↑	↓	↓	↑	↑	↓	↓
ASCL1^{hi} GNS (G523, G472)	↓	↓	↑	↑	—	—	—	—

Table S1. Summary of NDP/FZD4 manipulation phenotype on hNSC and GSC lines

Summary of observed effects on proliferation and sphere formation after knocking down or overexpressing NDP/ FZD4 in two hNSC, two ASCL1^{lo} GSC and two ASCL1^{hi} lines. (↑) indicates increase; (↓) indicates reduction; (—) no effect.

Table S2. Unique ASCL1^{lo} (G411) RNA-Seq identified hits

A list of the unique RNA-Seq hits identified after knocking down NDP in ASCL1^{lo} (G411) GSCs. The table represents expression comparison between scrambled and shNDP-C constructs, however; all included hits are validated to be significantly changed after knocking down NDP with both shNDP-A and shNDP-C constructs.

Table S3. Unique ASCL1^{hi} (G523) RNA-Seq identified hits

A list of the unique RNA-Seq hits identified after knocking down NDP in ASCL1^{hi} (G523) GSCs. The table represents expression comparison between scrambled and shNDP-C constructs, however; all included hits are validated to be significantly changed after knocking down NDP with both shNDP-A and shNDP-C constructs.

Table S4. Common RNA-Seq identified hits that overlap in the two lines after NDP knockdown

A list of the overlapping RNA-Seq hits identified after knocking down NDP in ASCL1^{lo} (G411) and ASCL1^{hi} (G523) GSC. For simplicity, the table includes a list of hits names and identifiers only, however; original expression values and fold changes are available in the full lists on GEO.

Table S5. Enriched gene sets in ASCL1^{lo} (G411) GSCs after *NDP* knockdown

A list of the ASCL1^{lo} (G411) unique gene sets from unbiased GSEA analysis of the RNA-Seq results after removing redundant sets. The table represents gene sets expression comparison

between scrambled and shNDP-C constructs, however; all included gene sets are validated to be significantly changed after *NDP* knockdown with shNDP-A and shNDP-C constructs.

Table S6. Enriched gene sets in ASCL1^{hi} (G523) GSCs after NDP knockdown

A list of the ASCL1^{hi} (G523) unique gene sets from unbiased GSEA analysis of the RNA-Seq results after removing redundant sets. The table represents gene sets expression comparison between scrambled and shNDP-C constructs, however; all included gene sets are validated to be significantly changed after *NDP* knockdown with shNDP-A and shNDP-C constructs.